Published in final edited form as:
Cell Metab. 2011 December 7; 14(6): 747–757. doi:10.1016/j.cmet.2011.11.006.

TGR5 activation inhibits atherosclerosis by reducing macrophage inflammation and lipid loading

Thijs W.H. Pols[1,*], **Mitsunori Nomura**[1,*], **Taoufiq Harach**[1], **Giuseppe Lo Sasso**[1], **Maaike H. Oosterveer**[1], **Charles Thomas**[1], **Giovanni Rizzo**[2], **Antimo Gioiello**[3], **Luciano Adorini**[2], **Roberto Pellicciari**[3], **Johan Auwerx**[1], and **Kristina Schoonjans**[1]

[1]Laboratory of Integrative and Systems Physiology (LISP), Ecole Polytechnique Fédérale de Lausanne, CH-1015 Lausanne, Switzerland. [2]Intercept Pharmaceuticals, New York, NY 10013, USA. [3]Dipartimento di Chimica e Tecnologia del Farmaco, Università di Perugia , Via del Liceo 1, 06123 Perugia, Italy.

SUMMARY

The G-protein coupled receptor TGR5 has been identified as an important component of the bile acid signaling network and its activation has been linked to enhanced energy expenditure and improved glycemic control. Here we demonstrate that TGR5 is expressed in macrophages, and that its activation by 6α-ethyl-23(S)-methyl-cholic acid (6-EMCA, INT-777), a semi-synthetic BA, inhibits pro-inflammatory cytokine production, an effect mediated by TGR5-induced cAMP signaling and subsequent NF-κB inhibition. TGR5 activation with the TGR5-specific agonist INT-777 was found to inhibit oxidized LDL uptake in macrophages, and attenuated atherosclerosis in $Ldlr^{-/-}Tgr5^{+/+}$ mice, but not in $Ldlr^{-/-}Tgr5^{-/-}$ double knockout mice. The inhibition of lesion formation was associated with decreased intraplaque inflammation and less plaque macrophage content. Furthermore, $Ldlr^{-/-}$ animals transplanted with bone marrow of $Tgr5^{-/-}$ mice did not show an inhibition of atherosclerosis by INT-777, further establishing an important role of leukocytes in INT-777-mediated inhibition of vascular lesion formation. Taken together, these data attribute a significant immune modulating function to TGR5 activation in the prevention of atherosclerosis, an important facet of the metabolic syndrome.

Keywords

Metabolic syndrome; Atherosclerosis; Inflammation; Macrophages; TGR5

INTRODUCTION

Bile acids (BAs), the main excretion products of cholesterol, are emerging as pleiotropic signaling molecules (Pols et al., 2010; Russell, 2009). Besides the well-established role of BAs in the activation of the nuclear receptor farnesoid X receptor (FXR) (Reviewed in (Modica et al., 2010)), BAs also activate the cell membrane receptor TGR5 (also known as GPBAR1 or GPR131) (Kawamata et al., 2003; Maruyama et al., 2002). Activation of TGR5 signaling controls several physiological pathways relevant to metabolic homeostasis, including the enhancement of energy expenditure through the induction of type 2 deiodinase

Corresponding author: Kristina Schoonjans, Ph.D Ecole Polytechnique Fédérale de Lausanne (EPFL) Laboratory of Integrative Systems and Physiology (LISP) SV IBI1; AI 1149 (Bâtiment AI); Station 19 CH-1015 Lausanne, Switzerland Phone : +41216931891; FAX: +41216939600 kristina.schoonjans@epfl.ch.
*These authors contributed equally

Europe PMC Funders Author Manuscripts

in brown adipocytes (Watanabe et al., 2006) and improvement of glucose tolerance through its commanding role on GLP-1 secretion from enteroendocrine cells (Thomas et al., 2009). In the liver, TGR5 activation protects against the development of hepatosteatosis (Katsuma et al., 2005; Thomas et al., 2009; Vassileva et al., 2010), while in the gallbladder, it modulates chloride and fluid secretion and stimulates smooth muscle relaxation (Keitel et al., 2009; Lavoie et al., 2010; Li et al., 2011).

Atherosclerosis is a chronic disorder of the vessel wall that underpins the development of important vascular diseases, such as coronary artery and cerebro-vascular disease (Rocha and Libby, 2009). The development and progression of atherosclerosis is enhanced by dyslipidemia and chronic inflammation, in which macrophages are proposed to play an important role (Rocha and Libby, 2009). The latter cells scavenge modified forms of LDL in the vessel wall, eventually resulting in foam cell formation and local production of cytokines and chemokines that initiate chronic inflammation of the vessel wall, one of the initial steps in the pathogenesis of atherosclerosis. Interestingly, TGR5 is expressed in several immune cells, such as monocytes, alveolar macrophages and Kupffer cells (Kawamata et al., 2003; Keitel et al., 2008), and it has been demonstrated that BAs modulate the inflammatory response in these cells. In agreement with these observations, it was recently shown that TGR5 activation inhibits the inflammatory response in the liver (Wang et al., 2011).

We hypothesized that TGR5 might have a role in the development of atherosclerosis and hence investigated the expression and function of TGR5 in macrophages, within the context of atherosclerosis. By using TGR5 loss- and gain-of function mouse models, in combination with a pharmacological approach to change TGR5 activity we here demonstrate an important role of TGR5 in the modulation of macrophage-mediated inflammation and in the development of atherosclerosis. Our work hence demonstrates that TGR5 may be a promising target for immune modulation, which could be exploited to prevent the development of atherosclerosis, an important facet of the metabolic syndrome.

RESULTS

The TGR5 agonist INT-777 inhibits macrophage inflammation

In our previous studies we showed that TGR5 activation protects mice from obesity and insulin resistance, two major hallmarks of the metabolic syndrome (Thomas et al., 2009; Watanabe et al., 2006). As chronic inflammation also significantly contributes to the progression of the metabolic syndrome, we initially explored the immune regulatory function of TGR5 *in vivo*. To do so, we injected mice intraperitoneally with LPS and took blood of these animals. Serum TNFα levels were increased 2 hrs after LPS, an effect that was more pronounced in $Tgr5^{-/-}$ animals as compared to $Tgr5^{+/+}$ animals (Figure S1A). We then assessed expression of TGR5 in several inflammatory cell populations and other tissues, isolated after thioglycollate-injection in the peritoneal cavity of C57Bl/6J mice. Cells were subsequently stained with specific antibodies allowing FACS-sorting of B-cells, T-cells, granulocytes and macrophages. *Tgr5* mRNA was detected in all tissues, including different immune cell populations, with various degrees of expression (Figure S1B). As previously reported, *Tgr5* was highly enriched in the gallbladder (Keitel et al., 2009; Vassileva et al., 2006). Most notably, *Tgr5* was expressed in the sorted $CD11b^{+}Gr^{-}$ macrophage population (Figure S1B), and could also be detected in several macrophage cell lines, and in cultured primary thioglycollate-elicited peritoneal macrophages (Figure S1C). Moreover, RAW264.7 cells transfected with a GFP-tagged human *Tgr5* construct showed that TGR5 localized to the cell membrane in macrophages as observed by confocal microscopy (Figure S1D).

We next treated cells with the TGR5-specific semi-synthetic BA, INT-777, and subsequently measured calcium flux and intracellular cAMP levels to investigate whether TGR5 is responsive in these cells. Consistent with reports in other cells (Keitel et al., 2009), INT-777 increased cAMP levels about 4-fold and induced a transient increase in cytosolic calcium in primary macrophages isolated from *Tgr5*$^{+/+}$ mice, which was not observed in INT-777-treated macrophages isolated from *Tgr5*$^{-/-}$ mice and confirmed the presence of functional agonist-responsive TGR5 in macrophages (Figure 1A and 1B).

We then stimulated primary macrophages from *Tgr5*$^{+/+}$ and *Tgr5*$^{-/-}$ mice with LPS. Gene expression levels of Tnfα and Il-1β (Figure 1C and S1E), as well as secreted TNFα protein (Figure 1D), were more induced in the *Tgr5*$^{-/-}$ relative to Tgr5$^{+/+}$ mice upon LPS stimulation. Conversely, the TNFα response to LPS was reduced in macrophages overexpressing TGR5, isolated from *Tgr5* transgenic mice, as compared to wildtype macrophages (Figure 1E and 1F). In addition, INT-777 treatment of *Tgr5*-transgenic macrophages resulted in an even further reduction of Tnfα mRNA levels as compared to wildtype macrophages (Figure S1F). These data suggest a critical role of TGR5 activation in modulating the cytokine response of macrophages. To further investigate whether TGR5 activation inhibits cytokine production of macrophages, we exposed RAW264.7 cells to INT-777 and subsequently stimulated cytokine production using LPS. LPS increased the mRNA levels of inflammatory cytokines in the cells with distinct kinetics for the different cytokines. Combined LPS-INT-777 treatment significantly attenuated the transient increase in mRNA levels for *Tnf*α, monocyte chemoattractant protein-1 (*Mcp-1*), *Il-6* and *Il-1*β (Figure 1G-1J).

TGR5 inhibits NF-κB activation via cAMP signaling

To gain more insight into the mechanism through which TGR5 activation suppressed inflammatory cytokine production, we assessed the activation of two major pro-inflammatory transcription factors, *i.e.* c-Jun, a component of AP-1, and nuclear factor κB (NF-κB) by Western blotting in RAW264.7 macrophages. As expected, total c-Jun levels as well as phosporylation of c-Jun was increased upon LPS stimulation of cells. TGR5 activation, however, did not modulate LPS-induced phosphorylation of c-Jun (Figure 2A). LPS also induced the nuclear translocation of p65, a hallmark of activation of NF-κB signaling (Figure 2A). In contrast to the phosphorylation of c-Jun, which remained unchanged, p65 translocation was significantly blunted by TGR5 activation with INT-777 (Figure 2A and 2B). This inhibitory effect of INT-777 was furthermore attenuated by the adenylyl cyclase inhibitor SQ22536, implying involvement of the cAMP pathway (Figure 2A and 2B). To get more mechanistic insight into the inhibitory effect of INT-777 on p65 translocation, we studied phosphorylation of IκBα, a substrate of IκB kinase (IKK), and NF-κB-p65 DNA binding activity to its response element. In line with the decreased nuclear NF-κB-p65 localization, INT-777 decreased both IκBα phosporylation and NF-κB-p65 DNA binding activity (Figure 2C, 2D and 2E).

We also measured NF-κB transcriptional activity by transfecting RAW264.7 macrophages with a NF-κB reporter plasmid containing the consensus NF-κB response element. In line with the findings on p65 nuclear translocation, NF-κB transcriptional activity was inhibited in LPS-treated macrophages in response to TGR5 activation or overexpression (Figure 2F), and was conversely increased upon TGR5 silencing (Figure 2G). In agreement with the cAMP-dependent effects of TGR5 on p65 nuclear translocation, SQ22536, as well as another adenylyl cyclase inhibitor, 2′5′-dideoxyadenosine, reversed the effects of TGR5 on NF-κB transcriptional activity (Figure 2H). Furthermore, INT-777 also inhibited inflammation in RAW264.7 cells stimulated with TNFα, demonstrating that the effect of INT-777 does not depend solely on LPS stimulation (Figure S2A and S2B). As β-arrestin-2 signaling has been implied in mediating anti-inflammatory effects of GPCRs (Oh et al.,

2010; Wang et al., 2011), we knocked down β-arrestin-2 in RAW264.7 cells using shRNA constructs (Figure S2C), but were unable to couple the anti-inflammatory effect of TGR5 activation to this molecule (Figure S2D and S2E).

To further explore the role of TGR5 in the inhibition of NF-κB we generated a mutant of the mouse TGR5 protein (TGR5-A217P). Human TGR5 containing this mutation is unable to activate cAMP-CREB signaling, presumably because the mutation is located in a loop important for G-protein interaction (Hov et al., 2010). Expression of both wildtype and mutant TGR5 protein was confirmed in CHO cells using our TGR5 antibody (Figure 3A-3I). TGR5-A217P did not enhance CREB activity in response to activation with INT-777, suggesting that it was incapable to induce cAMP signaling (Figure 3J). The TGR5-A217P mutant was then used to assess NF-κB activity in the presence of ectopically expressed p65. Interestingly, while the TGR5 wildtype protein robustly inhibited NF-κB transcriptional activity, the TGR5-A217P mutant failed to modulate NF-κB activity (Figure 3K), further establishing that the TGR5-cAMP-NF-κB pathway is critical for the inhibition of cytokine production in macrophages.

TGR5 activation inhibits oxidized LDL uptake

Besides inflammation, foam cell formation of macrophages is a key event in the initiation of atherosclerosis. It has been described that inhibition of NF-κB in macrophages reduces lipid loading and foam cell formation, which could suggest that TGR5 inhibits lipid loading via this pathway (Ferreira et al., 2007). To gain more insight into effects of TGR5 in lipid loading and foam cell formation, we investigated whether TGR5 modulates macrophage expression of scavenger receptor A (SR-A) and CD36, both involved in scavenging modified forms of LDL and foam cell formation (Febbraio et al., 2000; Suzuki et al., 1997). Interestingly, *Sr-a* as well as *Cd36* mRNA levels were higher in macrophages isolated from $Tgr5^{-/-}$ mice, relative to $Tgr5^{+/+}$ macrophages, and were reduced in $Tgr5^{+/+}$ macrophages in response to INT-777 (Figure 4A and 4B). In line with these observations, DiI-labeled oxidized LDL loading was decreased upon INT-777 exposure in macrophages of wildtype mice, but not in $TGR5^{-/-}$ mice (Figure 4C and 4D-4I), suggesting that TGR5 inhibits macrophage foam cell formation.

TGR5 activation inhibits atherosclerosis

The inhibitory effects of TGR5 activation on inflammation and oxidized LDL loading in macrophages suggested that TGR5 could attenuate the development of atherosclerosis. To investigate this hypothesis, we first crossbred the $Tgr5^{-/-}$ animals to atherosclerosis-susceptible $Ldlr^{-/-}$ mice to generate cohorts of $Ldlr^{-/-}Tgr5^{+/+}$ and $Ldlr^{-/-}Tgr5^{-/-}$ littermates. These cohorts were then used to further explore the effect of TGR5 activation on the development of atherosclerotic lesions. INT-777 was admixed to the atherogenic diet for 12 weeks at a dose sufficient to reach an intake of 30 mg/kg/day. Food intake was equal between the INT-777- and the control-treated groups as evaluated by 24 hrs home cage monitoring (data not shown). In line with previous studies (Thomas et al., 2009; Watanabe et al., 2006), treatment of INT-777 tended to reduce body weight and plasma glucose of $Ldlr^{-/-}Tgr5^{+/+}$, but not of $Ldlr^{-/-}Tgr5^{-/-}$ animals (Figure S3A and S3B). Furthermore, white blood cell populations were not significantly different between the genotypes or between control- and INT-777 treatment (Figure S3C).

We observed a significant reduction in vascular lesion formation in the aortic root of INT-777 treated $Ldlr^{-/-}Tgr5^{+/+}$ mice (Figure 5A-5C). This reduction, however, was not observed in $Ldlr^{-/-}Tgr5^{-/-}$ mice indicating that the protective effect of INT-777 was TGR5 dependent (Figure 5A-5E). Cholesterol is a major contributing factor to the development of atherosclerotic lesions and differences in plasma levels between control and INT-777 treated

Ldlr$^{-/-}$*Tgr5*$^{+/+}$ mice could potentially account for the observed effects. In line with the dysfunctional LDL uptake in *Ldlr*$^{-/-}$ mice, plasma cholesterol levels were extremely high in all experimental groups (Figure 5F). INT-777, however, did not affect the total levels of cholesterol or triglycerides in the two genotypes (Figure 5F and 5G). To get more insight into the action of INT-777 on vascular lesion formation, we also analyzed intraplaque inflammation by performing laser capture micro-dissection of the lesions in the aortic root (Figure S3D-S3F). In agreement with our previous observations, *Tnf*α and *Il-1*β mRNA levels were significantly decreased in plaques of INT-777 treated as compared to untreated *Ldlr*$^{-/-}$*Tgr5*$^{+/+}$ mice, whereas this effect of INT-777 was not observed in the *Ldlr*$^{-/-}$*Tgr5*$^{-/-}$ mice (Figure 5H and 5I). Interestingly, mRNA levels of the chemokines, *Mcp-1* and *Ccl5*, showed a similar response upon INT-777 treatment (Figure S3G and S3H). Further to this we analyzed plaque composition, by performing stainings for smooth muscle cell α-actin (ASMA) to detect smooth muscle cells (SMC), MAC3 to detect macrophages and Sirius red to stain collagen, which are major constituents of atherosclerotic lesions (Figure 6A-6L). Quantification of these stainings using image analysis software revealed no changes in SMC or collagen content, but indicated a reduced macrophage content in plaques derived from INT-777 treated *Ldlr*$^{-/-}$ *Tgr5*$^{+/+}$ mice as compared to untreated mice, whereas this reduction in macrophage content was not observed in *Ldlr*$^{-/-}$*Tgr5*$^{-/-}$ animals (Figure 6M-6O). Taken together, these data indicate that TGR5 activation inhibits vascular lesion formation, and that this process is associated with reduced intraplaque inflammation and decreased macrophage content.

INT-777 inhibits atherosclerosis through activation of TGR5 in leukocytes

To further confirm that the inhibition of atherosclerosis by INT-777 is mediated by leukocytes, we performed bone marrow transplantations to generate chimeric *Ldlr*$^{-/-}$ animals carrying bone marrow of either *Tgr5*$^{+/+}$ or *Tgr5*$^{-/-}$ mice. After the bone marrow transplantations, mice were fed an atherogenic diet for 8 weeks, with or without the addition of INT-777 at a dose of 30 mg/kg/day. Examination of genomic DNA, isolated from circulating white blood cells, indicated that the transplanted animals were highly chimeric as evidenced by the genotype observed in the *Tgr5* and *Ldlr* alleles (Figure 7A and 7B). This was furthermore confirmed by quantitatively measuring wildtype LDLR mRNA levels, which indicated that animals reached 70-95% of chimerism (Data now shown). Furthermore, analysis of white blood cell populations did not show any significant changes (Figure S4A). In addition, total plasma triglycerides and cholesterol were similar between the groups (Figure S4B and S4C). Upon assessment of atherosclerosis in the aortic root, a first observation was that, *Ldlr*$^{-/-}$ mice transplanted with bone marrow of *Tgr5*$^{+/+}$ mice developed less vascular lesions upon INT-777 treatment (Figure 7C -7G), which confirmed the robust inhibitory effect of INT-777 on the development of atherosclerosis (see Figure 5). This beneficial effect of INT-777 on plaque formation was totally lost in *Ldlr*$^{-/-}$ mice transplanted with *Tgr5*$^{-/-}$ bone marrow (Figure 7C-7G). Collectively, these data demonstrate that the effect of INT-777 on atherosclerosis is mediated through TGR5 activation in leukocytes.

DISCUSSION

In this study we demonstrate that activation of the membrane bile acid receptor TGR5 protects against the development of atherosclerosis. TGR5 is expressed in primary macrophages and is responsive to INT-777, a semisynthetic BA that specifically activates TGR5. The inhibition of cytokine production observed in INT-777 treated macrophages was dependent on the activation of the cAMP-NF-κB signaling pathway, and is in line with other observations demonstrating that cAMP inhibits NF-κB activity (Minguet et al., 2005; Parry and Mackman, 1997). Moreover, TGR5 reduced oxidized LDL uptake in macrophages,

which could contribute to the anti-atherogenic effects of INT-777. Most importantly, TGR5 activation inhibits the development of atherosclerosis in LDLR$^{-/-}$ mice fed a high cholesterol diet, which is in line with the attenuation of inflammation and oxidized LDL uptake observed in cultured macrophages. The inhibition of atherosclerosis in *Ldlr*$^{-/-}$ mice by TGR5 agonist treatment was associated with decreased intraplaque inflammation and caused by the activation of TGR5 in leukocytes, as concluded from experiments using bone marrow transplantations of *Tgr5*$^{-/-}$ and *Tgr5*$^{+/+}$ donors.

Macrophage inflammation is central to almost all aspects that contribute to the development of the atherosclerotic lesion, starting from the initiation of atherosclerosis up to plaque rupture that results in the induction of the coagulation cascade. In one of the initial reports on the identification of TGR5 as a BA sensor, the receptor was suggested to modulate the inflammatory response (Kawamata et al., 2003). In that study, BA treatment of rabbit alveolar macrophages increased cAMP production, and decreased phagocytic activity as well as TNFα secretion. In agreement with this, THP-1 cells overexpressing TGR5 showed similar effects in response to BAs, which was not observed in untransfected THP-1 cells. Similarly, a report in rat Kupffer cells demonstrated that BAs induce cAMP levels and decrease inflammatory cytokine production, suggestive for a role of TGR5 in this process (Keitel et al., 2008). In the current study, using primary macrophages isolated from mice with both TGR5 loss-of-function (*Tgr5*$^{-/-}$ mice) and gain-of-function (*Tgr5* overexpressing transgenic mice), we unequivocally demonstrate that TGR5 activation in macrophages potently inhibits inflammation by affecting cAMP- and NF-κB signaling. Furthermore, we show that the TGR5-cAMP-NF-κB signaling pathway modulates cytokine secretion and that several aspects of inflammation are perturbed in mice lacking TGR5, providing *in vivo* proof that TGR5 is an anti-inflammatory actor. These data are in line with a recent report that focuses on liver inflammation and demonstrates that TGR5 inhibits NF-κB inflammation in macrophages and Kupffer cells. In this study, it was suggested that the decrease in NF-κB activity in response to TGR5 activation involves increased β-arrestin-2 signaling (Wang et al., 2011). While β-arrestin-2 is known as an established regulatory component of GPCR signaling (Pierce et al., 2002), our data argue against a role for β-arrestin-2, and rather support a role of cAMP signaling to explain the anti-inflammatory activity of TGR5 activation.

In addition to reducing inflammation in macrophages, TGR5 activation seems to interfere, at least to a certain extent, with the uptake of modified lipoproteins in macrophages. Several endocytic pathways in macrophages can contribute to the focal buildup of cholesterol in arteries, which precedes atherosclerotic plaque formation (Rocha and Libby, 2009). In line with a contribution of macrophage lipid loading, we indeed observed a reduced expression of both *Cd36* and *Sr-a*, two receptors involved in the endocytosis of modified forms of LDL upon TGR5 activation. Although the inhibition of foam cell formation could in part be a consequence of reduced expression of *Sr-a* and *Cd36*, it could also be a consequence of the inhibition of NF-κB, which is known to inhibit foam cell formation (Ferreira et al., 2007). In this context, it is worth to mention that the atherogenic role of SR-A and CD36 has been challenged. This is exemplified by a report demonstrating that *Apoe*$^{-/-}$*Sr-a*$^{-/-}$ or *Apoe*$^{-/-}$*Cd36*$^{-/-}$ knockout mice did not show a reduction in atherosclerosis, despite the presence of reduced macrophage cholesterol ester accumulation (Moore et al., 2005). The precise implication of the downregulation of *Sr-a* and *Cd36*, as well as the inhibition of macrophage foam cell formation by TGR5 *in vitro* with regard to atherosclerotic plaque formation, therefore deserves further study.

Another interesting aspect relates to the nature of the plaque composition between control- and INT-777 treated animals. While most of the constituents of the atherosclerotic plaques were similar in both conditions, macrophage content was significantly reduced, as well as

the intraplaque inflammation assessed on isolated plaques of INT-777-treated animals. Since these parameters have a predictive function in the progression and destabilization of atherosclerotic plaques (Libby et al., 1996), treatment with TGR5 agonists is likely to result in a more stable plaque phenotype, and could hence be of relevance to reduce the risk of plaque rupture and occurrence of subsequent myocardial infarctions. Investigation of intraplaque expression of *Mcp-1* and *Ccl5* could indicate that the reduced expression of these chemokines contributed to decreased plaque macrophage content (Zernecke and Weber, 2010). What is most striking, however, is the critical contribution of the immune-modulating cells to the athero-protective action of TGR5. TGR5 activation is known to have a beneficial impact on various aspects of the metabolic syndrome by boosting energy metabolism and improving both glucose tolerance and lipid homeostasis (Reviewed in (Pols et al., 2010)). The insulinotropic hormone GLP-1, for instance, whose secretion is triggered by TGR5 activation in enteroendocrine cells (Katsuma et al., 2005; Thomas et al., 2008a), was recently shown to protect against atherosclerosis via a mechanism that involves cAMP induction in macrophages (Arakawa et al., 2010). Although it could be very well possible that such systemic effects could contribute to the athero-protective actions of TGR5 activation, the outcome of our bone-marrow transplant studies unequivocally establish the predominant role of TGR5 in leukocytes to explain this effect.

In view of the promise of TGR5 as a potential therapeutic target in the metabolic syndrome (Pols et al., 2010; Thomas et al., 2009; Thomas et al., 2008b; Watanabe et al., 2006), drug development efforts around this target are intense (Evans et al., 2009; Herbert et al., 2010). It is therefore expected that in addition to INT-777, several selective and potent non-BA TGR5 agonist will become available in the near future. Furthermore, many natural compounds have been described to activate TGR5, which include triterpenoid compounds of plant origin, such as oleanolic, ursolic and betulinic acid (Genet et al., 2010; Sato et al., 2007). With the prospect of using TGR5-specific natural and synthetic agonists to prevent and/or treat the metabolic syndrome in humans, our study suggests that such compounds also may have beneficial effects in the context of atherosclerosis, another important facet of the metabolic syndrome. Despite these potentially optimistic prospects, much more work is required to elucidate the pleiotropic actions of TGR5 and to assure that these beneficial effects observed in mice translate into humans. Importantly, atherosclerosis in humans is not identical to that observed in mouse models, and the beneficial effects of TGR5 activation in this animal model should be confirmed in human studies. Furthermore, the suppression of the inflammatory response, although beneficial within the context of chronic inflammatory diseases, such as atherosclerosis and the metabolic syndrome, may weaken host defense systems. As for any novel drug target, the development of TGR5 agonists therefore needs to proceed with caution and carefully balance the therapeutic benefits and potential side effects associated with the target (Lavoie et al., 2010; Li et al., 2011; Perides et al., 2010), reviewed in (Pols et al., 2010). Taken together, we demonstrate here that the activation of TGR5 prevents atherosclerotic lesion formation through an effect on leukocytes in $Ldlr^{-/-}$ mice, a commonly used mouse model of atherosclerosis. Inhibition of macrophage NF-κB signaling, as well as a reduction of macrophage foam cell formation, may both contribute to the protective effects of TGR5 activation in the context of the atherosclerotic plaque. In combination with its beneficial impact on energy homeostasis and glucose tolerance, the significant immune modulating function of TGR5 activation in the prevention of atherosclerosis further bolsters the importance of TGR5 as a potentially promising target to prevent and/or treat many facets of the metabolic syndrome.

EXPERIMENTAL PROCEDURES

Confocal imaging

For confocal imaging, cells were grown on Labtek II chamber slides (Nunc), and fixed using Shandon Formal Fixx (Thermo Scientific). Nuclei were subsequently stained with 4′,6-diamidino-2-phenylindole (DAPI), and cells were embedded using 1,4-diazabicyclo(2.2.2)octane (DABCO). Images were acquired using a LSM700 confocal microscope (Zeiss). Our TGR5 home-made antibody was raised in rabbits by immunization against the peptide 306 to 322 of mouse TGR5.

Lipid loading in macrophages

To investigate lipid loading, primary macrophages were cultured in medium containing 1% FCS in which 50 μg/ml DiI-OxLDL (BT-920; Biomedical Technologies) was added. After 8 hours of incubation, cells were fixed using Shandon Formal Fixx (Thermo Scientific), and confocal images were made. Alternatively, cells were washed with PBS and DiI-labeled oxidized LDL was extracted from cells using isopropanol after which fluorescence was measured in the Victor X4 (PerkinElmer) to quantifiy the amount of DiI-labeled oxidized LDL uptake.

Real-time qRT-PCR

RNA was isolated from cells using TRI Reagent (Ambion), after which cDNA was synthesized (Qiagen). Real-time qRT-PCR was performed using SYBR green (Roche) in the Lightcycler 480 II (Roche). All mRNA expression levels were corrected for expression of the housekeeping gene 36B4 or β2-microglobulin. Used primer sequences are available upon request.

Western blotting and NF-κB DNA binding activity

Western blotting was performed using antibodies against p65 (C-20), tubulin (B-7), and PARP-1 (N-20; Santa Cruz Biotechnology), C-Jun (9162) and phosphorylated-C-Jun (9261), IκBα (4814), phospho-IκBα (Ser32/36; 5A5; Cell Signaling) and HRP-labeled anti-rabbit secondary antibodies (Cell Signaling). The intensities of the protein bands were quantified using ImageJ software. NF-κB-p65 DNA binding activity was assessed by using a Trans Am transcription factor ELISA (Active Motif).

Reporter assays

RAW264.7 macrophages were transfected by electroporation using the Amaxa device (Lonza). Transfected vectors include the full-length mouse TGR5 (Watanabe et al., 2006), NF-κB reporter plasmid containing the NF-κB consensus sequence (Clontech), CMV-β-gal expression vector to correct for transfection efficiency (Clontech), Luciferase activity was measured using the luciferase assay system (Promega) in the Victor X4 (PerkinElmer). The CREB-luciferase reporter construct (Stratagene) contained 4 copies of the CRE enhancer sequence and was transfected in CHO cells with or without (mutant) TGR5 using JetPEI (Polyplus Transfection).

FACS sorting

Peritoneal cell populations isolated 5 days after intraperitoneal thioglycollate injection were FACS-sorted with the FACSAria II (BD Biosciences) using E-Fluor450-labeled anti-mouse CD45R, Phycoerythrin (PE)-Cy7-labeled anti-mouse CD11b, PE-labeled anti-mouse TCRβ, and Allophycocyanin (APC) anti-mouse GR1 (all from EBioscience) to separate different inflammatory cell populations present in the peritoneal cavity of 12 weeks-old C57Bl/6 mice after induction of inflammation by thioglycollate injection. The FcR was blocked with anti-

FcR antibodies (Fc γ RIIb/CD16-2 (derived from hybridoma 2.4G2)). Sorted cells were used for RNA isolation.

Bone marrow transplantation study

Mice used as bone marrow transplantation recipients were 8-10 weeks old LDLR$^{-/-}$ animals (strain B6.129S7-Ldlr^{tm1Her}/J; Jackson Research) that were subjected to total body X-irradiation of 850 Rad (RS2000 Irradiator) split into two exposures after NK cells were depleted by injecting the mice with the monoclonal PK136 antibody. TGR5$^{-/-}$ or TGR5$^{+/+}$ littermates aged 4-6 weeks were used as bone marrow donors. After four weeks of recovery, which included treatment with Baytril (Bayer) and Dafalgan (Bristol-Myers Squibb), mice were fed the atherogenic diet (TD94059; Harlan) containing 30mg/kg INT-777 for 8 weeks. Chimerism was assessed by isolating genomic DNA from white blood cells 8 weeks after transplantation using the following primers for the LDLR gene: Primer 1 (common): 5′-CCATATGCATCCCCAGTCTT-3′; Primer 2 (wt): 5′-AATCCATCTTGTTCAATGGCC-3′; Primer 3 (Mut): 5′-GCGATGGATACACTCACTGC-3′). TGR5 deletion in the white blood cells was confirmed using the following primers: Primer A (Del): 5′-GATGGCTGAGAGGCGAAG-3′, Primer B: (common) 5′-AGAGCCAAGAGGGACAATCC-3′, Primer C (Wt): 5′-TGGGTGAGTGGAGTCTTCCT-3′. Primers for LDLR (Primer 1 and 2) as well as a calibration curve consisting of mixed DNA of LDLR$^{-/-}$ and wildtype animals allowed qRT-PCR reactions to quantify chimerism. LDLR gene levels were corrected using primers against the myogenin gene (Primer 1: 5′-TTACGTCCATCGTGGACAGC-3′ and Primer 2: 5′-TGGGCTGGGTGTTAGCCTTA-3′).

Laser capture microdissection

Laser capture micro-dissection of lesions was performed on unfixed frozen sections of the aortic root using the Autopix laser capture microdissection device (Arcturus). Tissue used for RNA isolation using the PicoPure RNA isolation kit (Arcturus) was derived from pooling captured tissue from 8 consecutive sections of each lesion, after which cDNA was synthesized using the VILO cDNA synthesis kit (Qiagen). Lesions of three representative animals per groups were used for laser capture microdissection.

Immunohistochemistry stainings and quantification

Antibodies against MAC3 (Pharmingen) and ASMA (1A4; Dako) were used for immunohistochemistry to detect lesion macrophages and smooth muscle cells. A Sirius red staining was performed to stain collagen. The FcR was blocked with anti-FcR antibodies (Fc γ RIIb/CD16-2 (derived from hybridoma 2.4G2)). The Mac3 staining was visualized using Vectastain Elite ABC Peroxidase kit Rat IgG (Vector) and NovaRED substrate (Vector), the Asma staining was visualized using KIT Mouse IgG (Immpress) and DAB substrate (Sigma). Positive surface area's were determined using ImageJ software using a color deconvolution plug-in.

Cell culture

Primary macrophages were isolated from the peritoneal cavity 5 days after thioglycollate injection, plated in culture dishes, and washed 24 hrs after plating to discard non-macrophage populations. Serum-starved macrophages were stimulated with INT-777 in the presence of 0.1% BSA. The calcium flux was measured using a Fluo-4 fluorescent probe (Molecular Probes) in the Victor X4 (PerkinElmer). Intracellular cAMP was measured 1 hour after addition of INT-777 using a cAMP chemoluminescent immunoassay kit (Applied Biosystems). SQ22536 and 2′, 5′-dideoxyadenosine were bought from Sigma. TNFα levels

were quantified using the Mouse TNFα ELISA Ready-SET-Go! (eBioscience). RAW264.7 cells were transfected using electroporation (Lonza) with the TGR5 silencing construct (Origene). β-arrestin-2 shRNA or control shRNA constructs were cloned into the pENTR/U6 vector (Invitrogen); sequences are available upon request.

Animals, biochemistry and atherosclerosis assessment

All animal studies were performed according to regulations issued by the Swiss government. TGR5 genetic models were described earlier (Thomas et al., 2009). The mice were backcrossed for 10 generations with the C57BL/6J strain, yielding congenic C57BL/6J *Tgr5*$^{-/-}$ animals. The controls that were used were littermates in all experiments. Mice were sacrificed 12 weeks after the initiation of the atherogenic diet (TD94059; Harlan), after which the heart and aorta were perfused with PBS and subsequently fixed (Shandon Formal Fixx, Thermo Scientific). Atherosclerosis was assessed by an Oil-red-O staining of the aortic root and quantified using MetaMorph software. Biochemistry parameters were measured using appropriate kits in the COBAS C111 (Roche). For the *in vivo* LPS study, mice were intraperitoneally injected with 100 μg LPS, blood was taken from the tail vein. TNFα levels were quantified using the Mouse TNFα ELISA Ready-SET-Go! (eBioscience). Blood cell counts were determined using the Advia2120 (Siemens Healthcare Diagnostics).

Statistical analysis

The student *t* test was used to calculate the statistical significance. In case of multiple testing (i.e. the comparison of more than two groups), this test was preceded by the ANOVA test. $P<0.05$ was considered statistically significant. Results represent the mean ± SEM.

Supplementary Material

Refer to Web version on PubMed Central for supplementary material.

Acknowledgments

We thank Pablo José Fernández-Marcos and Mark Pruzanski for helpful discussions and reagents. We thank Amandine Moriot-Signorino-Gelo, Norman Moullan, Sabrina Bichet and Thibaud Clerc for excellent technical assistance. We are grateful to the center of phenogenomics (UDP) for assisting our experiments. We acknowledge the Swiss National Science Foundation (SNF 31003A_125487), European Research Council, Nestlé and the Ecole Polytechnique Fédérale de Lausanne for funding. J.A. is the Nestle Chair in Energy Metabolism. T.W.H.P. is supported by a long-term fellowship from FEBS, and M.N. is supported by a doctoral fellowship from AXA.

REFERENCES

Arakawa M, Mita T, Azuma K, Ebato C, Goto H, Nomiyama T, Fujitani Y, Hirose T, Kawamori R, Watada H. Inhibition of monocyte adhesion to endothelial cells and attenuation of atherosclerotic lesion by a glucagon-like peptide-1 receptor agonist, exendin-4. Diabetes. 2010; 59:1030–1037. [PubMed: 20068138]

Evans KA, Budzik BW, Ross SA, Wisnoski DD, Jin J, Rivero RA, Vimal M, Szewczyk GR, Jayawickreme C, Moncol DL, et al. Discovery of 3-aryl-4- isoxazolecarboxamides as TGR5 receptor agonists. J Med Chem. 2009; 52:7962–7965. [PubMed: 19902954]

Febbraio M, Podrez EA, Smith JD, Hajjar DP, Hazen SL, Hoff HF, Sharma K, Silverstein RL. Targeted disruption of the class B scavenger receptor CD36 protects against atherosclerotic lesion development in mice. J Clin Invest. 2000; 105:1049–1056. [PubMed: 10772649]

Ferreira V, van Dijk KW, Groen AK, Vos RM, van der Kaa J, Gijbels MJ, Havekes LM, Pannekoek H. Macrophage-specific inhibition of NF-kappaB activation reduces foam-cell formation. Atherosclerosis. 2007; 192:283–290. [PubMed: 16938301]

Genet C, Strehle A, Schmidt C, Boudjelal G, Lobstein A, Schoonjans K, Souchet M, Auwerx J, Saladin R, Wagner A. Structure-activity relationship study of betulinic acid, a novel and selective

TGR5 agonist, and its synthetic derivatives: potential impact in diabetes. J Med Chem. 2010; 53:178–190. [PubMed: 19911773]

Herbert MR, Siegel DL, Staszewski L, Cayanan C, Banerjee U, Dhamija S, Anderson J, Fan A, Wang L, Rix P, et al. Synthesis and SAR of 2-aryl-3-aminomethylquinolines as agonists of the bile acid receptor TGR5. Bioorg Med Chem Lett. 2010; 20:5718–5721. [PubMed: 20801037]

Hov JR, Keitel V, Laerdahl JK, Spomer L, Ellinghaus E, ElSharawy A, Melum E, Boberg KM, Manke T, Balschun T, et al. Mutational characterization of the bile acid receptor TGR5 in primary sclerosing cholangitis. PLoS One. 2010; 5:e12403. [PubMed: 20811628]

Katsuma S, Hirasawa A, Tsujimoto G. Bile acids promote glucagon-like peptide-1 secretion through TGR5 in a murine enteroendocrine cell line STC-1. Biochem Biophys Res Commun. 2005; 329:386–390. [PubMed: 15721318]

Kawamata Y, Fujii R, Hosoya M, Harada M, Yoshida H, Miwa M, Fukusumi S, Habata Y, Itoh T, Shintani Y, et al. A G protein-coupled receptor responsive to bile acids. J Biol Chem. 2003; 278:9435–9440. [PubMed: 12524422]

Keitel V, Cupisti K, Ullmer C, Knoefel WT, Kubitz R, Haussinger D. The membrane-bound bile acid receptor TGR5 is localized in the epithelium of human gallbladders. Hepatology. 2009; 50:861–870. [PubMed: 19582812]

Keitel V, Donner M, Winandy S, Kubitz R, Haussinger D. Expression and function of the bile acid receptor TGR5 in Kupffer cells. Biochem Biophys Res Commun. 2008; 372:78–84. [PubMed: 18468513]

Lavoie B, Balemba OB, Godfrey C, Watson CA, Vassileva G, Corvera CU, Nelson MT, Mawe GM. Hydrophobic bile salts inhibit gallbladder smooth muscle function via stimulation of GPBAR1 receptors and activation of KATP channels. J Physiol. 2010; 588:3295–3305. [PubMed: 20624794]

Li T, Holmstrom SR, Kir S, Umetani M, Schmidt DR, Kliewer SA, Mangelsdorf DJ. The G protein-coupled bile acid receptor, TGR5, stimulates gallbladder filling. Mol Endocrinol. 2011; 25:1066–1071. [PubMed: 21454404]

Libby P, Geng YJ, Aikawa M, Schoenbeck U, Mach F, Clinton SK, Sukhova GK, Lee RT. Macrophages and atherosclerotic plaque stability. Curr Opin Lipidol. 1996; 7:330–335. [PubMed: 8937525]

Maruyama T, Miyamoto Y, Nakamura T, Tamai Y, Okada H, Sugiyama E, Itadani H, Tanaka K. Identification of membrane-type receptor for bile acids (M-BAR). Biochem Biophys Res Commun. 2002; 298:714–719. [PubMed: 12419312]

Minguet S, Huber M, Rosenkranz L, Schamel WW, Reth M, Brummer T. Adenosine and cAMP are potent inhibitors of the NF-kappa B pathway downstream of immunoreceptors. Eur J Immunol. 2005; 35:31–41. [PubMed: 15580656]

Modica S, Gadaleta RM, Moschetta A. Deciphering the nuclear bile acid receptor FXR paradigm. Nucl Recept Signal. 2010; 8:e005. [PubMed: 21383957]

Moore KJ, Kunjathoor VV, Koehn SL, Manning JJ, Tseng AA, Silver JM, McKee M, Freeman MW. Loss of receptor-mediated lipid uptake via scavenger receptor A or CD36 pathways does not ameliorate atherosclerosis in hyperlipidemic mice. J Clin Invest. 2005; 115:2192–2201. [PubMed: 16075060]

Oh DY, Talukdar S, Bae EJ, Imamura T, Morinaga H, Fan W, Li P, Lu WJ, Watkins SM, Olefsky JM. GPR120 is an omega-3 fatty acid receptor mediating potent anti-inflammatory and insulin-sensitizing effects. Cell. 2010; 142:687–698. [PubMed: 20813258]

Parry GC, Mackman N. Role of cyclic AMP response element-binding protein in cyclic AMP inhibition of NF-kappaB-mediated transcription. J Immunol. 1997; 159:5450–5456. [PubMed: 9548485]

Perides G, Laukkarinen JM, Vassileva G, Steer ML. Biliary acute pancreatitis in mice is mediated by the G-protein-coupled cell surface bile acid receptor Gpbar1. Gastroenterology. 2010; 138:715–725. [PubMed: 19900448]

Pierce KL, Premont RT, Lefkowitz RJ. Seven-transmembrane receptors. Nat Rev Mol Cell Biol. 2002; 3:639–650. [PubMed: 12209124]

Pols TW, Noriega LG, Nomura M, Auwerx J, Schoonjans K. The bile acid membrane receptor TGR5 as an emerging target in metabolism and inflammation. J Hepatol. 2010; 54:1263–1272. [PubMed: 21145931]

Rocha VZ, Libby P. Obesity, inflammation, and atherosclerosis. Nat Rev Cardiol. 2009; 6:399–409. [PubMed: 19399028]

Russell DW. Fifty years of advances in bile acid synthesis and metabolism. J Lipid Res. 2009; 50(Suppl):S120–125. [PubMed: 18815433]

Sato H, Genet C, Strehle A, Thomas C, Lobstein A, Wagner A, Mioskowski C, Auwerx J, Saladin R. Anti-hyperglycemic activity of a TGR5 agonist isolated from Olea europaea. Biochem Biophys Res Commun. 2007; 362:793–798. [PubMed: 17825251]

Suzuki H, Kurihara Y, Takeya M, Kamada N, Kataoka M, Jishage K, Ueda O, Sakaguchi H, Higashi T, Suzuki T, et al. A role for macrophage scavenger receptors in atherosclerosis and susceptibility to infection. Nature. 1997; 386:292–296. [PubMed: 9069289]

Thomas C, Auwerx J, Schoonjans K. Bile acids and the membrane bile acid receptor TGR5--connecting nutrition and metabolism. Thyroid. 2008a; 18:167–174. [PubMed: 18279017]

Thomas C, Gioiello A, Noriega L, Strehle A, Oury J, Rizzo G, Macchiarulo A, Yamamoto H, Mataki C, Pruzanski M, et al. TGR5-mediated bile acid sensing controls glucose homeostasis. Cell Metab. 2009; 10:167–177. [PubMed: 19723493]

Thomas C, Pellicciari R, Pruzanski M, Auwerx J, Schoonjans K. Targeting bile-acid signalling for metabolic diseases. Nat Rev Drug Discov. 2008b; 7:678–693. [PubMed: 18670431]

Vassileva G, Golovko A, Markowitz L, Abbondanzo SJ, Zeng M, Yang S, Hoos L, Tetzloff G, Levitan D, Murgolo NJ, et al. Targeted deletion of Gpbar1 protects mice from cholesterol gallstone formation. Biochem J. 2006; 398:423–430. [PubMed: 16724960]

Vassileva G, Hu W, Hoos L, Tetzloff G, Yang S, Liu L, Kang L, Davis H, Hedrick J, Lan H, et al. Gender-dependent effect of Gpbar1 genetic deletion on the metabolic profiles of diet-induced obese mice. J Endocrinol. 2010; 3:225–232. [PubMed: 20354075]

Wang YD, Chen WD, Yu D, Forman BM, Huang W. The G-Protein-coupled bile acid receptor, Gpbar1 (TGR5), negatively regulates hepatic inflammatory response through antagonizing nuclear factor kappa light-chain enhancer of activated B cells (NF-kappaB) in mice. Hepatology. 2011; 54:1421–1432. [PubMed: 21735468]

Watanabe M, Houten SM, Mataki C, Christoffolete MA, Kim BW, Sato H, Messaddeq N, Harney JW, Ezaki O, Kodama T, et al. Bile acids induce energy expenditure by promoting intracellular thyroid hormone activation. Nature. 2006; 439:484–489. [PubMed: 16400329]

Zernecke A, Weber C. Chemokines in the vascular inflammatory response of atherosclerosis. Cardiovasc Res. 2010; 86:192–201. [PubMed: 20007309]

Europe PMC Funders Author Manuscripts

Europe PMC Funders Author Manuscripts

HIGHLIGHTS

- TGR5 triggers a cAMP-dependent pathway in primary macrophages
- Activation of TGR5 attenuates NF-κB signaling
- TGR5 activation reduces macrophage lipid loading and inflammation
- TGR5 activation in macrophages inhibits atherosclerosis

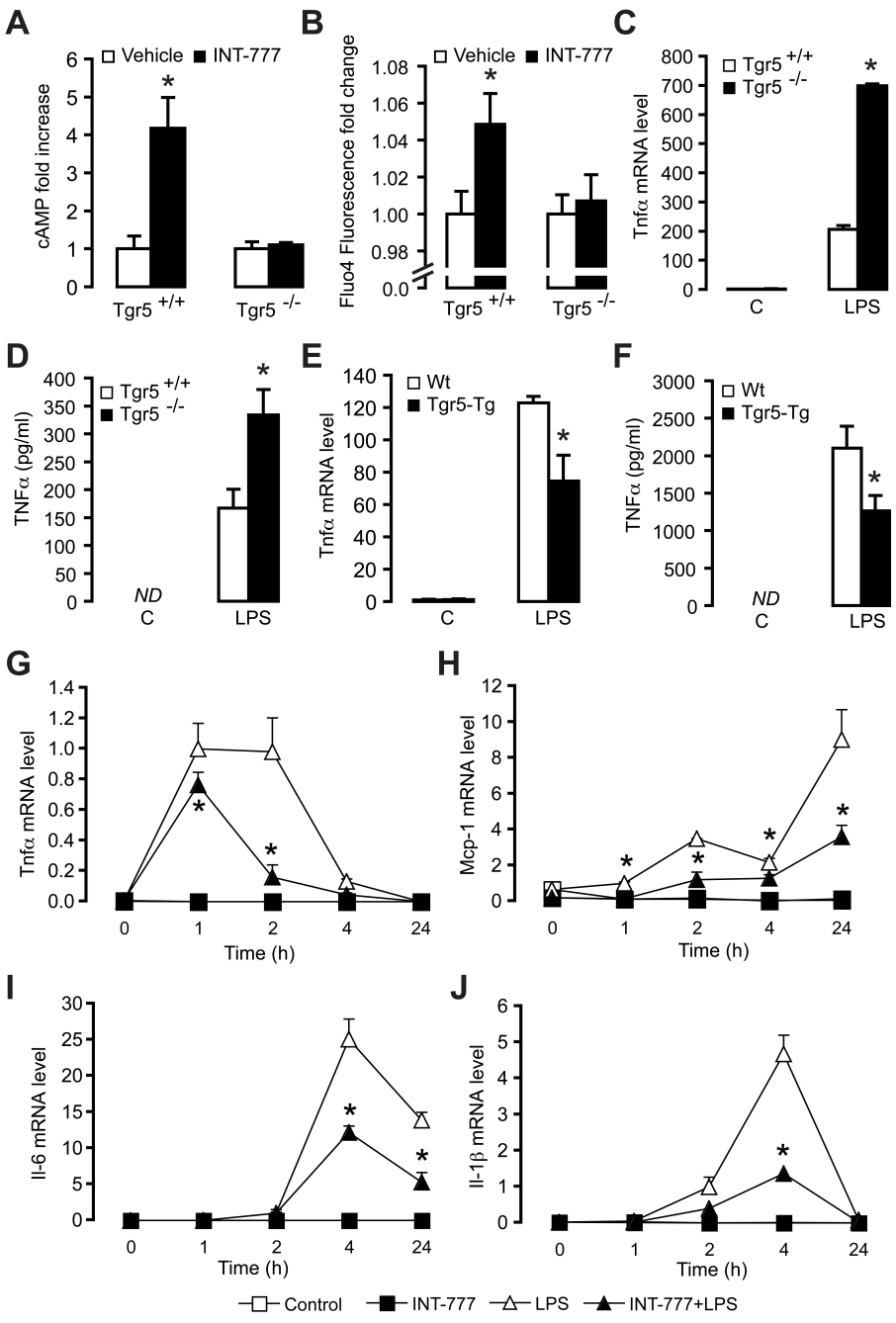

Figure 1. The TGR5 agonist INT-777 inhibits macrophage inflammation

(A) cAMP induction in primary macrophages isolated from *Tgr5*$^{-/-}$ and *Tgr5*$^{+/+}$ mice measured 1 hr after stimulation with vehicle (white bars) or 3 μM INT-777 (black bars); (n=3). **(B)** Intracellular calcium flux in primary macrophages isolated from *Tgr5*$^{-/-}$ and *Tgr5*$^{+/+}$ mice measured 30 sec after addition of 3 μM INT-777 (n=3). **(C and D)** mRNA expression **(C)** and protein secretion **(D)** of TNFα in primary macrophages isolated from *Tgr5*$^{+/+}$ (white bars) or *Tgr5*$^{-/-}$ mice (black bars) in response to stimulation with 100 ng/ml LPS for 6 hrs (n=3). **(E and F)** mRNA level **(E)** and protein level **(F)** of TNFα in macrophages isolated from *Tgr5*-Tg mice (black bars) and wildtype mice (white bars)

stimulated with 100 ng/ml LPS for 6 hrs in combination with treatment of 30 μM INT-777. **(G-J)** *Tnfα* **(G),** *Mcp-1* **(H),** *Il-6* **(I)**, and *Il-1β* **(J)** cytokine mRNA in response to 100 ng/ml LPS (triangles) or not stimulated (squares) treated with 30 μM INT-777 (black) or control-treated (white) in RAW264.7 macrophages (n=3). All conditions are present at all timepoints. Results represent the mean ± SEM. * Statistically significant, $P<0.05$.

Europe PMC Funders Author Manuscripts

Europe PMC Funders Author Manuscripts

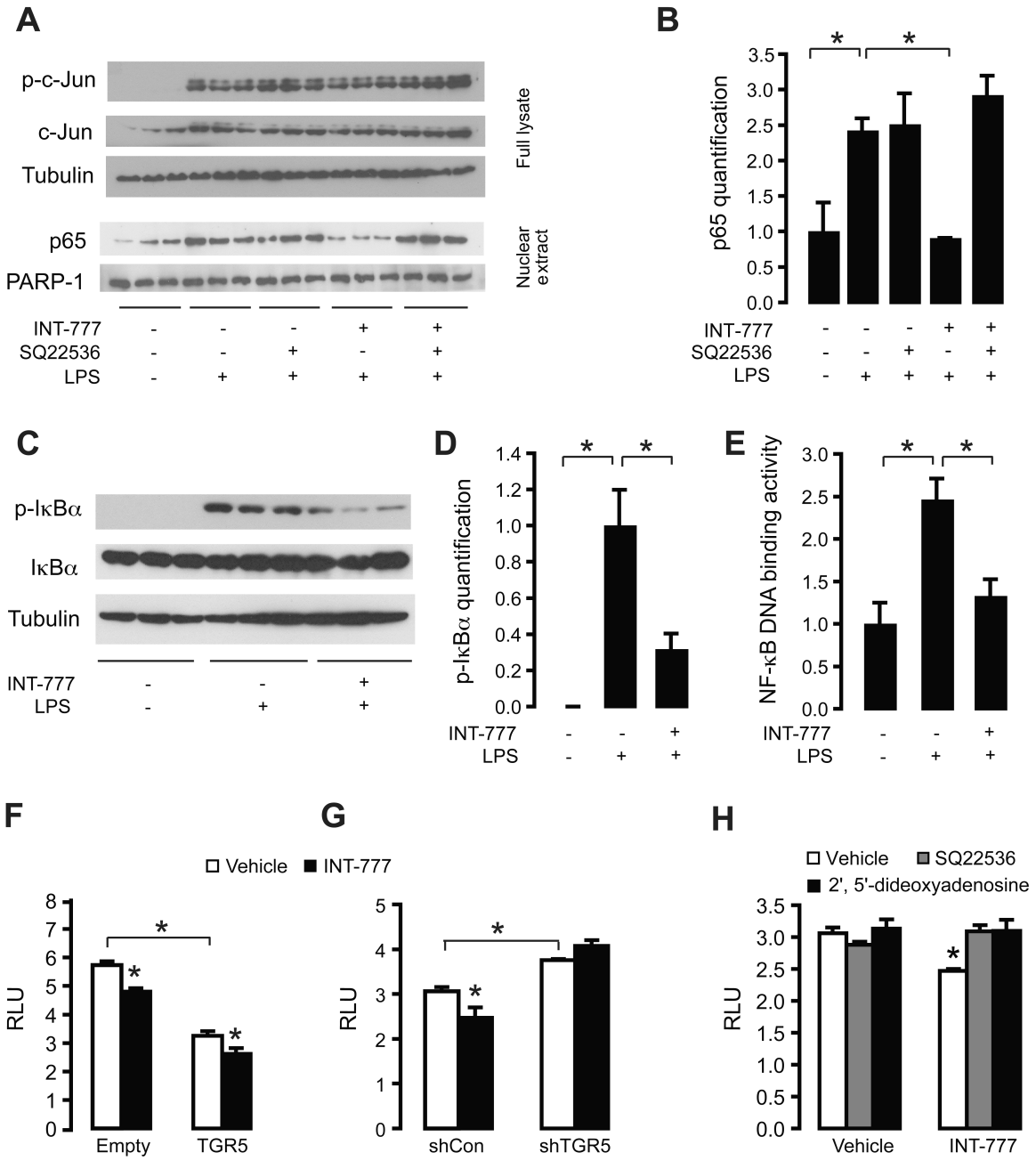

Figure 2. TGR5 activation inhibits NF-κB activation via cAMP signaling

(A) Western blot of C-Jun, phosphorylated c-Jun (P-C-Jun) with tubulin as loading control, and NF-κB p65 western blot of nuclear extract with PARP-1 as loading control of RAW264.7 macrophages treated with 100 ng/ml LPS for 3 hrs in combination with 100 μM SQ22536 and 30 μM INT-777 (n=3). **(B)** Quantification of western blot band intensity of p65 corrected for the intensity of PARP-1 using image analysis software. **(C)** Western blot of phosphorylated IκBα, total IκBα, and tubulin as loading control of lysate of RAW264.7 macrophages treated with 100 ng/ml LPS for 1 hr in combination with 30 μM INT-777 (n=3). **(D)** Quantification of western blot band intensity of IκBα corrected for the intensity

of tubulin using image analysis software. **(E)** NF-κB-p65 binding activity to its DNA response element after 3 hours LPS stimulation. **(F-H)** LPS-induced (6 hrs) NF-κB transcriptional activity in RAW264.7 macrophages electroporated with the NF-κB reporter plasmid in combination with electroporation of TGR5 **(F)** or shTGR5 **(G)** in the presence of 30 μM INT-777 (black bars) or vehicle (white bars) (n=3) **(H)** LPS-induced NF-κB transcriptional activity in RAW264.7 macrophages electroporated with the NF-κB reporter plasmid in combination with 30 μM INT-777 treatment or vehicle in the presence of 100 μM SQ22536 (grey bars), 20 μM 2′, 5′-dideoxyadenosine (black bars) or control conditions (white bars) (n=3). Results represent the mean ± SEM. * Statistically significant, $P<0.05$.

Europe PMC Funders Author Manuscripts

Europe PMC Funders Author Manuscripts

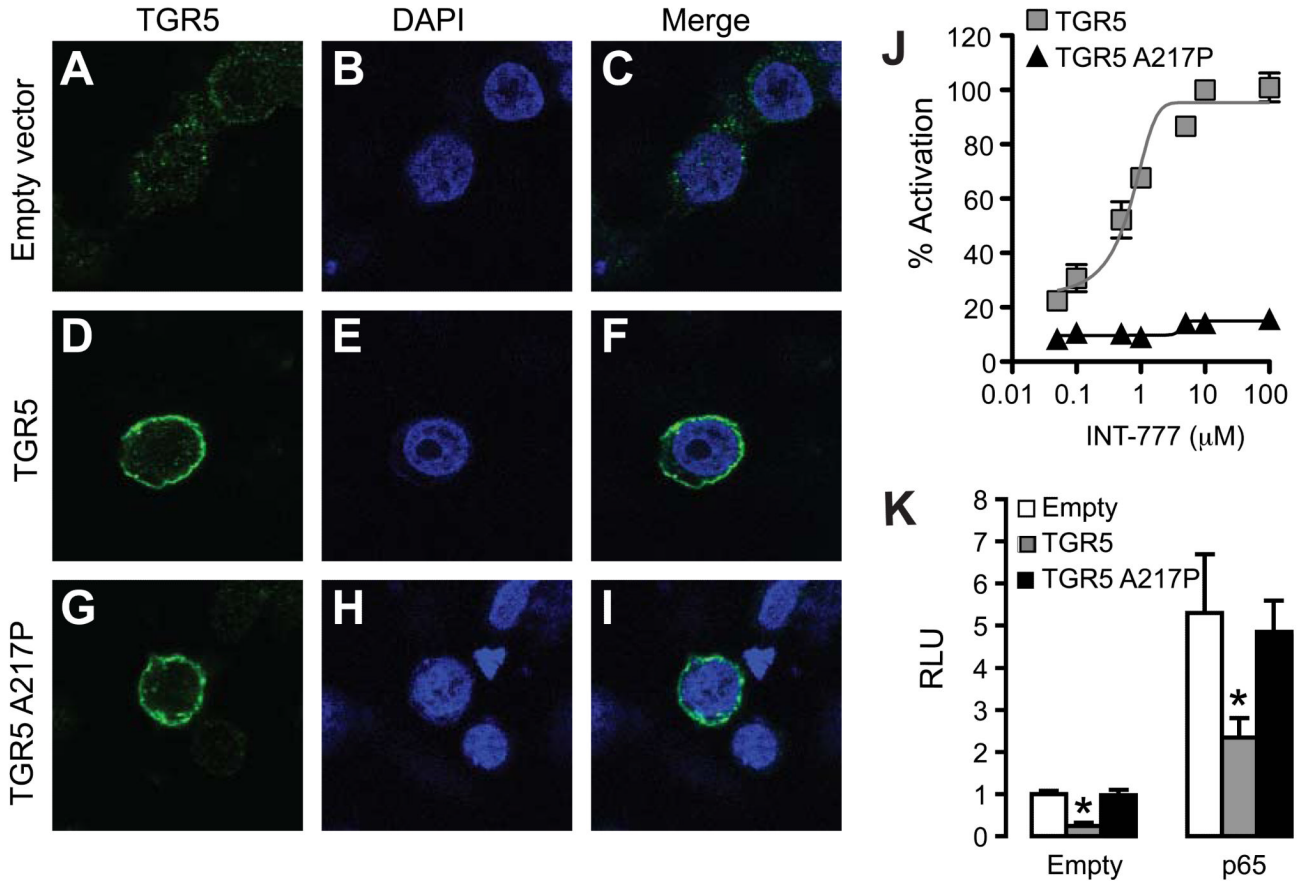

Figure 3. The TGR5 mutant TGR5-A217P, defective in inducing cAMP signaling, fails to inhibit NF-κB activity

(A-I) Confocal images of empty vector **(A-C),** mouse TGR5 **(D and F),** and TGR5-A217P mutant **(G-I)** -transfected CHO cells stained with DAPI **(B, E, H)**, stained for TGR5 **(A, D, G)** or shown as merged images **(C, F, I). (J)** CREB transcriptional activity in CHO cells transfected with both a CRE reporter and TGR5 wildtype (grey squares) or TGR5-A217P mutant (black triangles) in response to INT-777 (n=3). **(K)** NF-κB transcriptional activity in CHO cells transfected with the NF-κB reporter plasmid in combination with empty vector (white bars), TGR5 (grey bars) and TGR5-A217P (black bars) with or without NF-κB p65 co-transfection (n=3). Results represent the mean ± SEM. * Statistically significant, P<0.05.

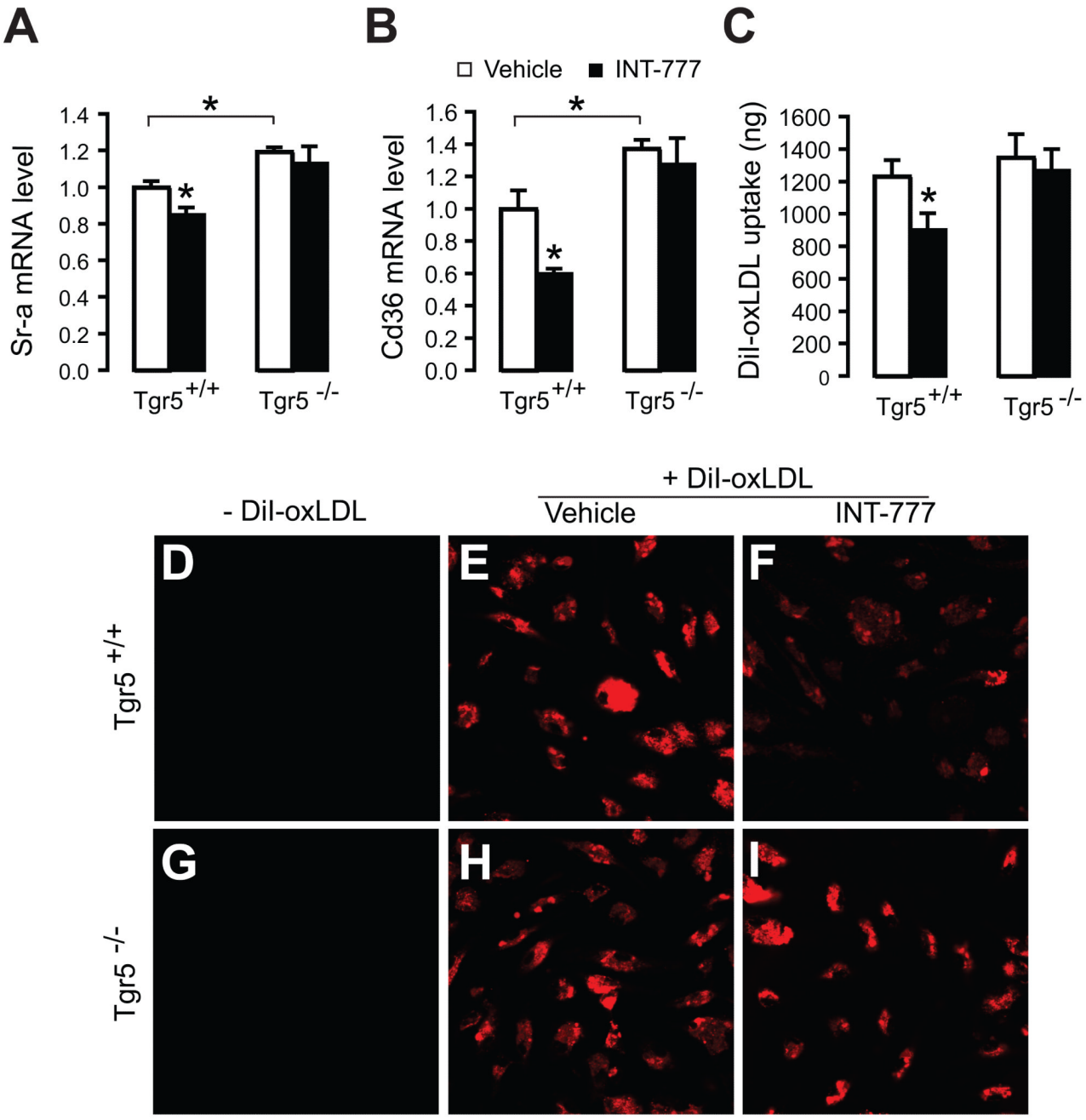

Figure 4. TGR5 inhibits oxidized LDL uptake

(A and B) *Sr-a* **(A)** and *Cd36* **(B)** mRNA expression in macrophages isolated from *Tgr5*$^{+/+}$ and *Tgr5*$^{-/-}$ mice in response to INT-777 treatment (black bars) or control-treated (white bars; n=3). **(C)** Fluorescence of DiI-labeled oxidized LDL extracted from macrophages isolated from *Tgr5*$^{+/+}$ and *Tgr5*$^{-/-}$ mice in response to INT-777 (black bars) or control conditions (white bars; n=3) **(D-I)** Confocal fluorescent images of macrophages from *Tgr5*$^{+/+}$ **(D, E, F)** and *Tgr5*$^{-/-}$ **(G, H, I)** mice treated with DiI-labeled oxidized LDL **(E, F, H, I)** in combination with INT-777 treatment **(F, I)**. Results represent the mean ± SEM. * Statistically significant, P<0.05.

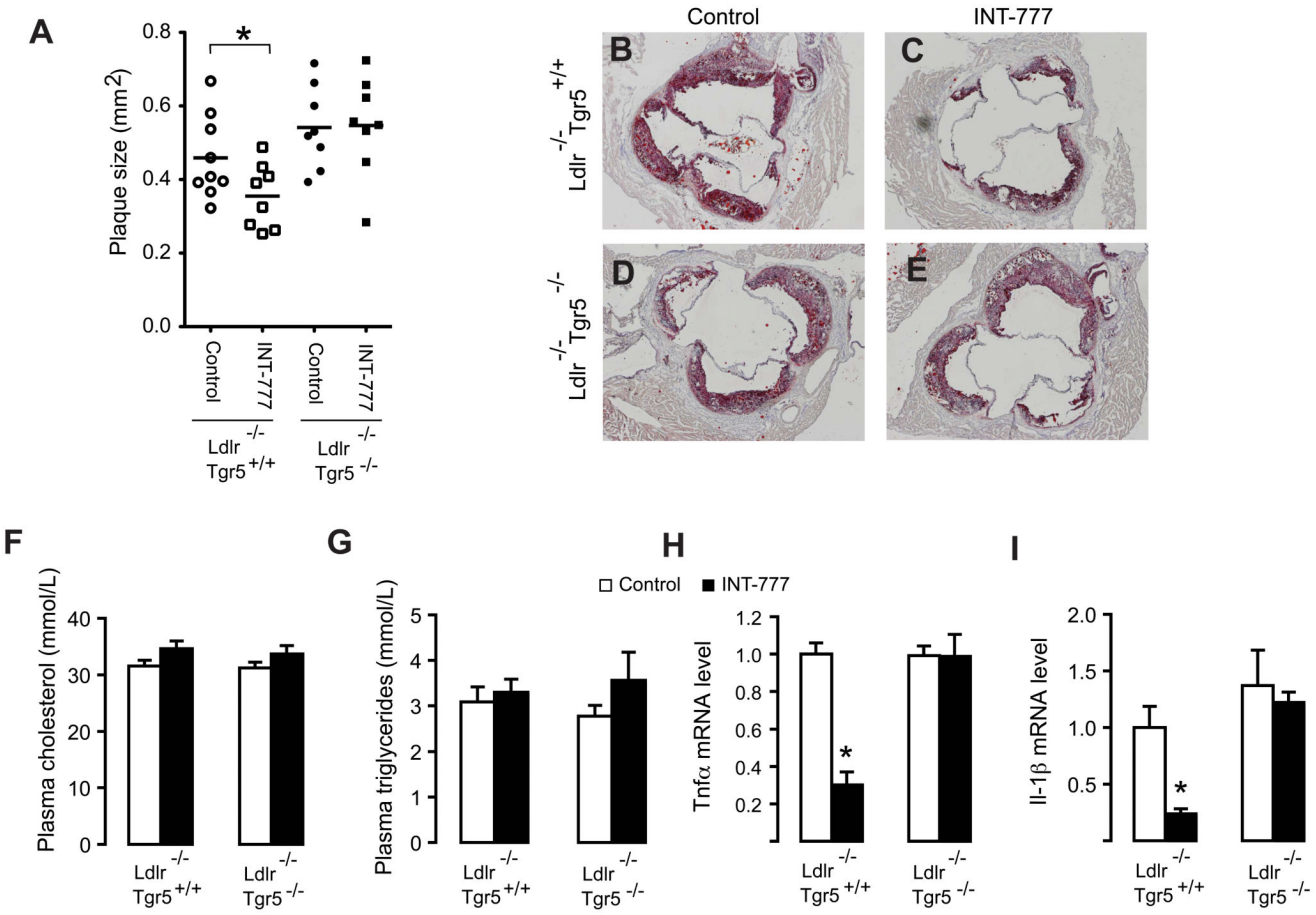

Figure 5. TGR5 activation inhibits atherosclerosis

(A) Plaque size in the aortic root of *Ldlr*$^{-/-}$ *Tgr5*$^{+/+}$ (white symbols) and *Ldlr*$^{-/-}$ *Tgr5*$^{-/-}$ animals (black symbols) treated with INT-777 (squares) or control-treated (circles) (n=8-9). **(B-E)** Oil-red-O staining of atherosclerotic lesions in the aortic root of *Ldlr*$^{-/-}$ *Tgr5*$^{+/+}$ **(B and C)** or *Ldlr*$^{-/-}$ *Tgr5*$^{-/-}$ animals **(D and E)** treated with INT-777 **(C and E)** or control-treated **(B and D)**. **(F and G)** Plasma cholesterol **(F)** and triglycerides **(G)** of *Ldlr*$^{-/-}$ *Tgr5*$^{+/+}$ and *Ldlr*$^{-/-}$ *Tgr5*$^{-/-}$ animals treated with INT-777 (black bars) or control-treated (white bars; n=8-9). **(H-I)** mRNA levels of **(H)** *Tnfα* and **(I)** *Il-1β* in aortic root lesions captured by laser capture micro-dissection of *Ldlr*$^{-/-}$ *Tgr5*$^{+/+}$ and *Ldlr*$^{-/-}$ *Tgr5*$^{-/-}$ animals treated with INT-777 (black bars) or control-treated (white bars; n=3). Results represent the mean ± SEM. * Statistically significant, P<0.05.

Europe PMC Funders Author Manuscripts

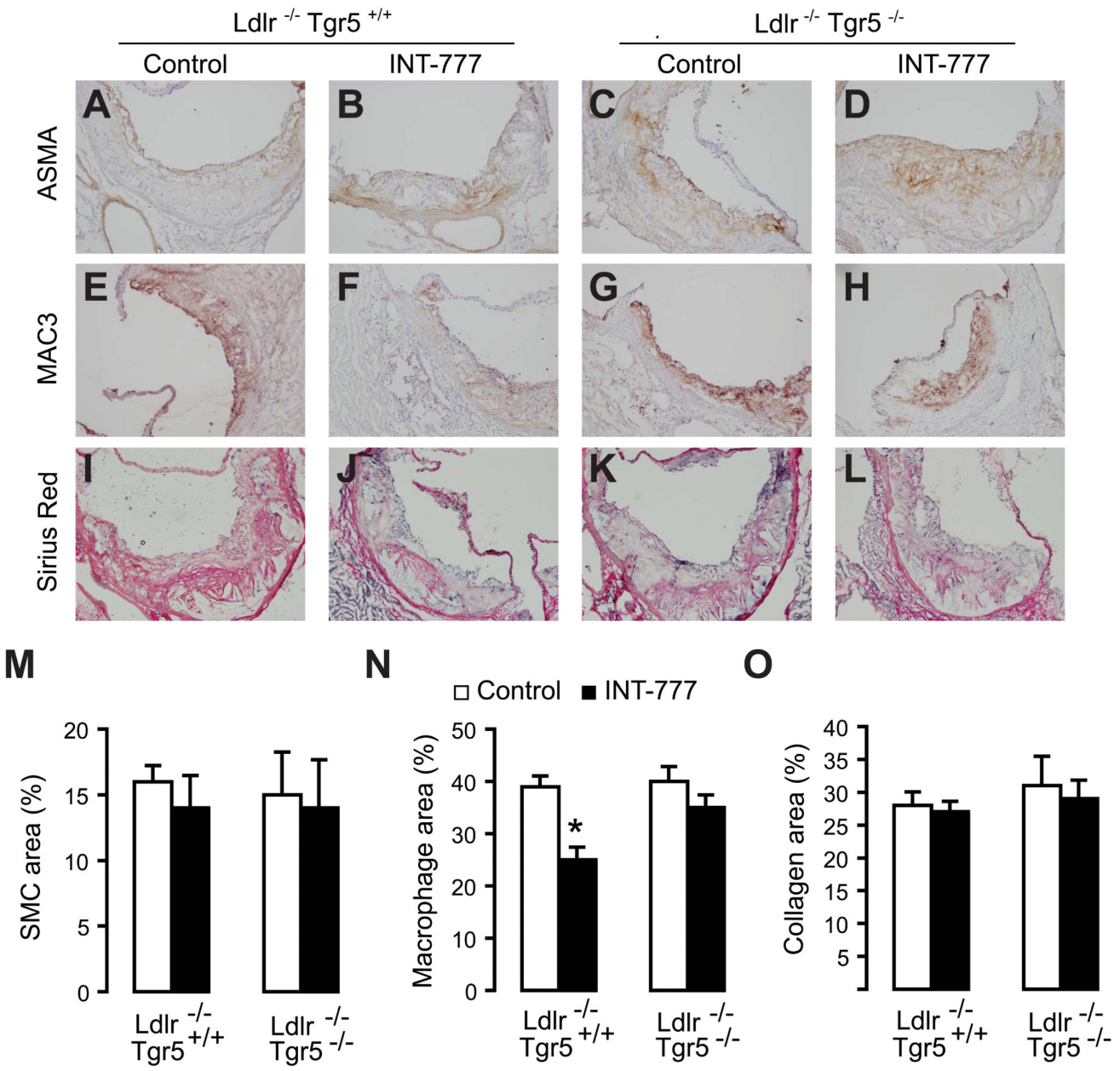

Figure 6. TGR5 modulates plaque macrophage content

(A-D) ASMA staining, **(E-H)** MAC3 staining **(I-L)** Sirius red staining to detect smooth muscle cells, macrophages and collagen, respectively, in aortic root lesions of *Ldlr*$^{-/-}$ *Tgr5*$^{-/-}$ and *Ldlr*$^{-/-}$ *Tgr5*$^{+/+}$ animals treated with or without INT-777. **(M-O)** Quantification of ASMA **(M)**, MAC3 **(N)** and Sirius red **(O)** staining area using image analysis software of aortic root lesions of *Ldlr*$^{-/-}$ *Tgr5*$^{-/-}$ and *Ldlr*$^{-/-}$ *Tgr5*$^{+/+}$ animals treated with (black bars) or without INT-777 (white bars; n=8-9). Results represent the mean ± SEM. * Statistically significant, P<0.05.

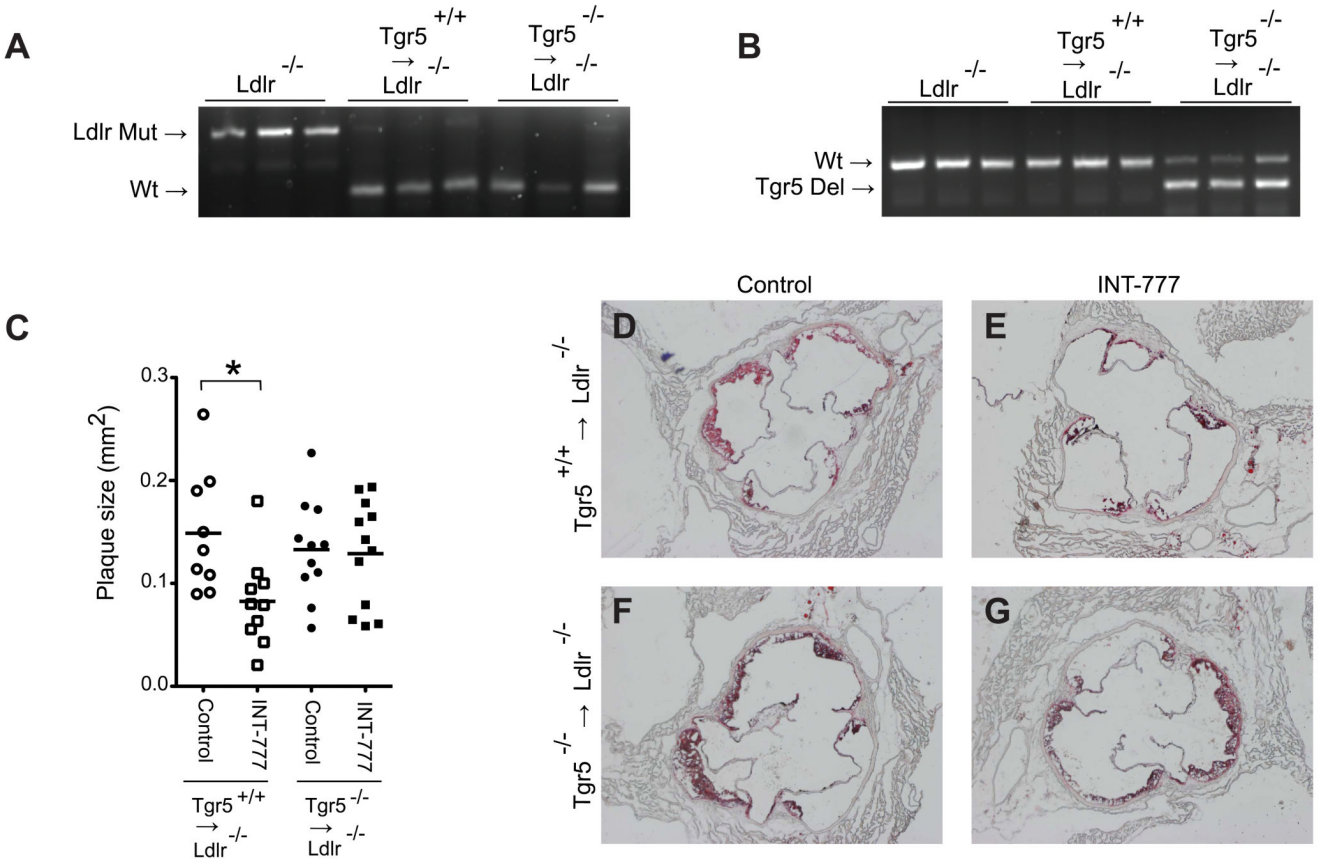

Figure 7. INT-777 inhibits atherosclerosis through activation of TGR5 in leukocytes

(A and B) PCR products showing the genotype of the *Ldlr* **(A)** and *Tgr5* **(B)** locus in genomic DNA isolated from circulating white blood cells of $Ldlr^{-/-}$ animals as well as $Ldlr^{-/-}$ animals transplanted with $Tgr5^{+/+}$ and $Tgr5^{-/-}$ bone marrow. **(C)** Plaque size in the aortic root of $Ldlr^{-/-}$ animals transplanted with $Tgr5^{+/+}$ (white symbols) or $Tgr5^{-/-}$ bone marrow (black symbols) treated with INT-777 (squares) or control-treated (circles) (n=9-12). **(D-G)** Oil-red-O staining of atherosclerotic lesions in the aortic root of $Ldlr^{-/-}$ animals carrying $Tgr5^{+/+}$ **(D and E)** or $Tgr5^{-/-}$ bone marrow **(F and G)** treated with INT-777 **(E and G)** or control-treated **(D and F)**. * Statistically significant, P<0.05.